JACS
JOURNAL OF THE AMERICAN CHEMICAL SOCIETY

Article

pubs.acs.org/JACS

Smart Stimuli-Responsive Spherical Nanostructures Constructed from Supramolecular Metallodendrimers via Hierarchical Self-Assembly

Li-Jun Chen,[†] Guang-Zhen Zhao,[†] Bo Jiang,[†] Bin Sun,[†] Ming Wang,[⊥] Lin Xu,[†] Jiuming He,[‡] Zeper Abliz,[‡] Hongwei Tan,[∥] Xiaopeng Li,[⊥] and Hai-Bo Yang*[,†]

[†]Shanghai Key Laboratory of Green Chemistry and Chemical Processes, Department of Chemistry, East China Normal University, Shanghai 200062, P. R. China

[‡]Institute of Materia Medica, Chinese Academy of Medical Sciences and Peking Union Medical College, Beijing 100050, P. R. China

[∥]Department of Chemistry, Beijing Normal University, Beijing 100050, P. R. China

[⊥]Department of Chemistry and Biochemistry, Texas State University, San Marcos, Texas 78666, United States

Supporting Information

ABSTRACT: In this article, we present the design and construction of a series of supramolecular poly(benzyl ether) metallodendrimers featuring a well-defined hexagonal metallacycle at their cores via coordination-driven self-assembly. It was found that the second generation metallodendrimer **3c** was able to hierarchically self-assemble into the regular vesicle-like structures. These nanoscale vesicles were monodisperse in shape and relatively monodisperse in size as detected in SEM, TEM, AFM, and DLS experiments. Notably, this kind of hierarchically formed vesicle-like nanostructure adopted a discrete metallacycle as the main skeleton, which is obviously different from many previous reports of nanoscale spherical architectures. Moreover, such supramolecular vesicle-like structures could encapsulate some fluorescent molecules, like BODIPY and SRB, etc. By taking advantage of the dynamic nature of metal−ligand bonds, the disassembly and reassembly of the hexagonal cavity core could be reversibly controlled by the addition and removal of bromide ions, resulting in the transition from the vesicles to micelles. Thus, the controlled release of fluorescence dye was successfully realized by the halide-induced vesicles−micelles transition. These findings not only enrich the library of supramolecular metallodenrimers but also provide a new avenue to the construction of novel "smart" nanomaterials, which have potential application in functional molecules delivery and release.

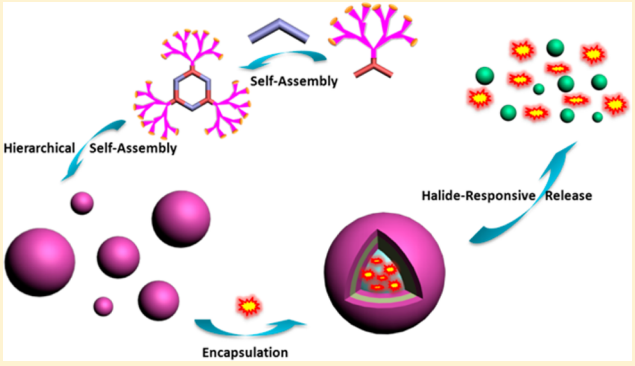

INTRODUCTION

Dendrimers are highly branched, three-dimensional macromolecules that contain several dendritic wedges extending outward from an internal core.[1] During the past few decades, the increasing attention has been paid to the design and synthesis of diverse dendrimers not only because of their aesthetically pleasing structures but also due to their wide applications in various areas such as host−guest chemistry, material science, and membrane chemistry, etc.[2] Recently, the considerable attention has turned to the construction of supramolecular dendritic architectures held together by noncovalent interactions.[3] Among the multiple noncovalent interactions, metal−ligand coordination bonds are particularly attractive as a result of their relatively stronger bond energy (ca. 15−50 kcal/mol) and highly directional and predictable nature. Thus, metal−ligand coordination provides a highly efficient strategy to prepare the desired supramolecular metallodendrimers. Because of their obvious synthetic advantages such as few steps, fast, and facile construction of the final products and inherent self-correcting, defect-free assembly, metal−ligand coordination bonds have been widely used in the construction of supramolecular metallodendrimers since the pioneering work by Newkome[4] and Balzani[5] in the early 1990s. Moreover, the incorporation of metals expands the potential application of the resulting metallodendrimers to catalysis, supramolecular redox sensors, biological mimetics, and light-harvesting antennae, etc.[6]

Recently, fabrication of functional nanostructures through self-assembly of small molecular building blocks via a "bottom-up" strategy has evolved to be one of the most attractive topics within supramolecular chemistry and materials science.[7] In particular, the design and construction of stimuli-responsive "smart" nanoscale materials are of special interest because of

Received: January 7, 2014
Published: March 31, 2014

Scheme 1. Self-Assembly of [G-0]−[G-2] 120° Dendritic Donors 1a−c and Acceptor 2 into the Hexagonal Metallodendrimers 3a−c

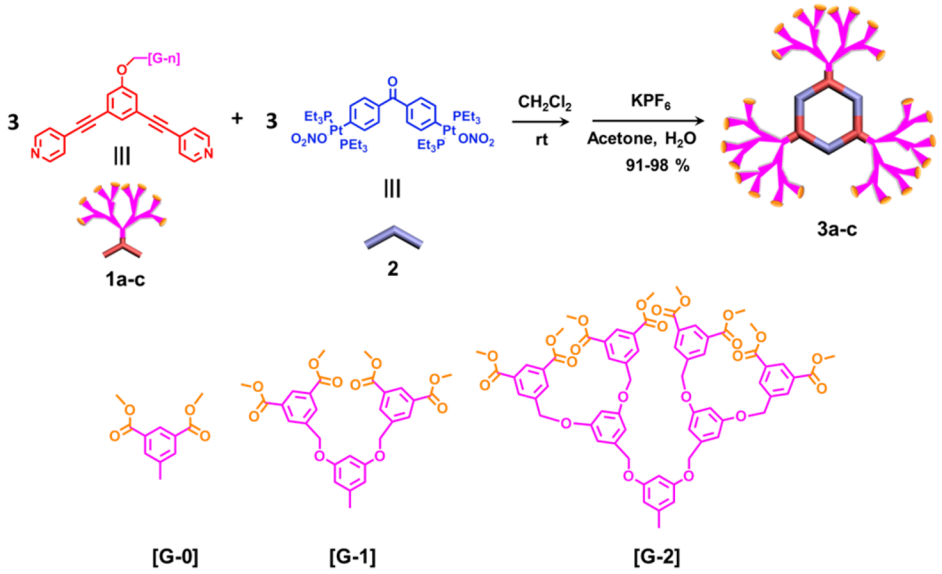

their various applications in the fields of catalysis, sensors, and drug delivery, etc.[8] However, it is still a big challenge to prepare the well-defined smart nanostructures with the higher order through a well-controlled self-assembly. As one essential skeleton, dendrimers have been explored as a class of fundamental building blocks to fabricate functional nanoscale systems. For instance, physically thermoreversible organogels based on dendrons or dendrimers with different functionality have been reported.[9] It should be noted that, despite the rapidly growing body of literature on self-assembly of dendrimers, there are very few successful examples of cavity-cored dendrons or dendrimers that can form the ordered supramolecular aggregates or functional nanostructures.[10]

Over the past decades, coordination-driven self-assembly, which is based on metal−ligand coordination interaction, has evolved to be a well-established methodology for the construction of novel metallosupramolecular structures from two-dimensional (2-D) polygons to three-dimensional (3-D) cages, prisms, and polyhedra.[11,12] Based on this strategy, a great number of functional supramolecular polygons and polyhedra have been successfully prepared, which exhibit the extensive applications in the area of host−guest chemistry, catalysis, bioengineering, etc.[13,14] Recently, a new family of supramolecular cavity-cored metallodendrimers with the predetermined shape, geometry, and symmetry have been constructed by the proper choice of dendritic building blocks and complementary precursors with predefined angles and symmetry via coordination-driven self-assembly.[15] Notably, Fréchet-type poly(benzyl ether) dendrons were usually employed in the construction of such cavity-cored metallodendrimers. However, because of their relatively weak intermolecular actions ($\pi-\pi$ stacking and van der Waals forces), few studies about the hierarchical self-assembly behavior of these cavity-cored metallodendrimers were performed. More recently, peripherally dimethyl isophthalate (DMIP) functionalized poly(benzyl ether) dendrons were found to be able to self-assemble into the stable organogel driven by the $\pi-\pi$ stacking, CH$-\pi$ interactions, and nontypical hydrogen bonds.[16] Thus, we envisioned that this kind of dendrons could be utilized to prepare new functionalized dendritic metallacycles that may hierarchically self-assemble into the ordered nanostructures by taking advantage of the orthogonality of metal−ligand coordination and other weak interaction including $\pi-\pi$ stacking, CH$-\pi$ interactions, and nontypical hydrogen bonds. Such hierarchically formed architectures may exhibit unique properties and functions that are not displayed by their individual components. Additionally, the presence of a molecular cavity could bring an additional dimension to the final supramolecular aggregates. Combining the properties of dendrimers with the dynamic nature of supramolecular metallacycles may offer the final obtained nanostructures a great potential for extracting, storing, and releasing compounds such as pharmaceuticals.

Herein, we designed and constructed a series of peripherally DMIP-functionalized poly(benzyl ether) metallodendrimers **3a−c** featuring a well-defined hexagonal metallacycle at their cores via coordination-driven self-assembly. Such hexagonal metallodendrimers were found to hierarchically self-assemble into the nanoscale, monodisperse vesicle-like structures mainly driven by multiple intermolecular interactions (e.g., $\pi-\pi$ stacking, CH$-\pi$ interactions, and hydrogen bonds) imposed by peripherally DMIP-functionalized poly(benzyl ether) dendrons. The further investigation revealed that transitions from the vesicles to micelles stimulated by the addition of Br^- were obtained, which was caused by the halide-induced disassembly of the hexagonal cavity core. More importantly, by taking advantage of the halide-induced vesicles−micelles transition, the encapsulation and controlled release of fluorescent molecules by such vesicle-like nanostructures were successfully realized. To the best of our knowledge, this study presented one of very few successful examples of smart stimuli-responsive spherical nanostructures constructed from supramolecular metallodendrimers via hierarchical self-assembly.

RESULTS AND DISCUSSION

Synthesis and Characterization. The self-assembled [G-0]−[G-2] metallodendritic hexagons **3a−c** were prepared by simply mixing the donor ligand **1a−c**[10c] with the 120° diplatinum(II) acceptor **2**[12a] in a 1:1 ratio in CH_2Cl_2, respectively. With the addition of aqueous solution of KPF_6,

dx.doi.org/10.1021/ja500152a | J. Am. Chem. Soc. 2014, 136, 5993−6001

pale-yellow precipitates of hexagonal metallodendrimers **3a**–**c** were obtained (Scheme 1). In each case, the product was centrifuged and washed several times with water. The pale-yellow solid was then dissolved in CD_2Cl_2 for ^1H, $^{31}P\{^1H\}$, and ^{13}C NMR analysis.

Multinuclear NMR (^1H, ^{31}P, and ^{13}C) analysis of [G-0]–[G-2] assemblies **3a**–**c** exhibited very similar characteristics, which supported the formation of discrete, highly symmetric hexagonal dendritic metallacycles. For instance, each $^{31}P\{^1H\}$ NMR spectrum of the [G-0]–[G-2] assemblies **3a**–**c** displayed a sharp singlet (ca. 13.4–13.6 ppm) shifted upfield from the starting platinum acceptor **2** by ~6.2 ppm (Figure 1). This

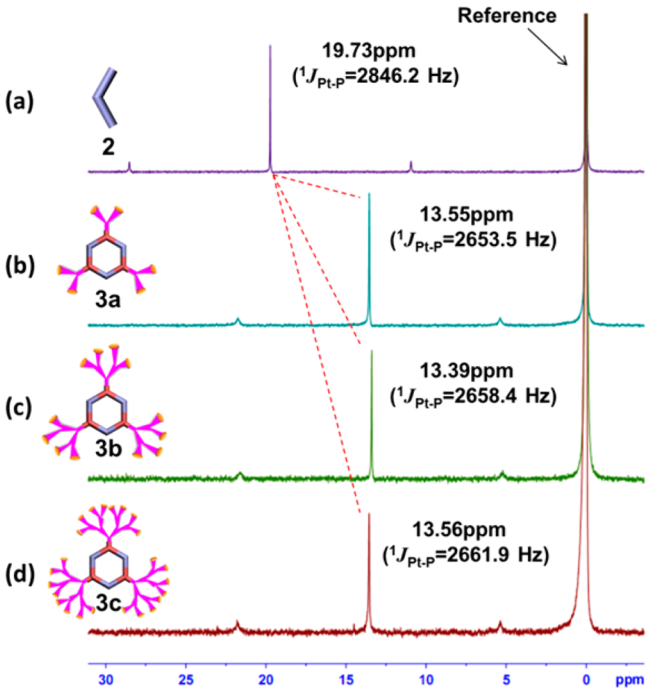

Figure 1. The ^{31}P NMR spectra (161.9 MHz, in CD_2Cl_2, 298 K) of acceptor **2** (a), [G-0] self-assembled hexagon **3a** (b), [G-1] self-assembled hexagon **3b** (c), and [G-2] self-assembled hexagon **3c** (d).

change, as well as the decrease in coupling of flanking ^{195}Pt satellites (ca. ΔJ = −187.4 to −192.7 Hz), is consistent with the electron back-donation from the platinum atoms. In the ^1H NMR spectrum of each assembly, the α and β hydrogen atoms of the pyridine rings displayed downfield shifts (α-H, 0.05–0.06 ppm; β-H, 0.42–0.43 ppm) due to the loss of electron density that occurs upon coordination of the pyridine-N atom with the Pt(II) metal center (Figures S1–S3). The sharp NMR signals in ^1H, $^{31}P\{^1H\}$, and ^{13}C NMR spectra along with the solubility of these species ruled out the formation of oligomers. Further characterization by 2-D spectroscopic techniques (2-D ^1H–^1H NOESY), in which the presence of cross peaks between the signals of the PEt_3 protons and the pyridine protons were observed, was in agreement with the formation of the discrete hexagonal metallodendrimers (Figures S4–S6).

Mass spectrometric studies of the hexagonal metallodendrimers **3a**–**c** were performed by using the electrospray ionization mass spectrometry (ESI-TOF-MS) technique, which has been recognized as an effective tool to determine the molecular composition of supramolecular architectures since it is able to keep the assembly intact to the maximum extent during the ionization process. The mass spectrum of **3c** (8456.15 Da) was selected as a representative example. As shown in Figure 2, the mass spectrum of **3c** revealed three main

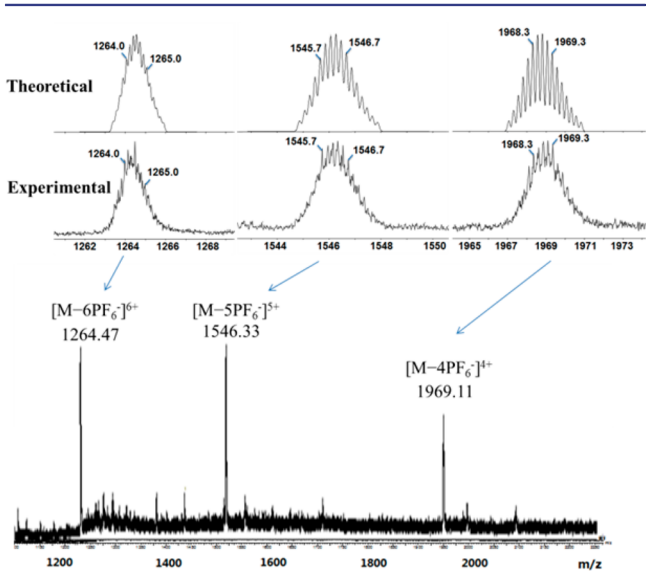

Figure 2. Theoretical and experimental ESI-TOF-MS spectrum of [G-2] dendritic hexagon **3c**.

peaks at m/z = 1231.54, 1546.33, and 1969.11, corresponding to different charge states resulted from the loss of hexafluorophate counterions [M−6PF_6^-]$^{6+}$, [M−5PF_6^-]$^{5+}$, and [M−4PF_6^-]$^{4+}$, respectively, where M represents the intact assembly. Further investigation disclosed that each isotope pattern of these peaks was in good agreement with the corresponding simulated result. It should be noted that no obvious superimposed fragments, overlapping isomers, or conformers of the assembly were found in the full spectrum, thus supporting that only [3 + 3] hexagonal metallodendrimer **3c** was formed in this study. Similarly, in the case of hexagons **3a** and **3b**, the peaks that agreed well with the corresponding simulated isotope patterns of were found in the mass spectra of **3a** and **3b**, respectively (Figures S29 and S31). Thus, the investigation of ESI-TOF-MS spectrometry provided the further support for the existence of the hexagonal metallodendrimers **3a**–**c**.

Unfortunately, all attempts to grow X-ray quality single crystals of the hexagonal metallodendrimers **3a**–**c** have proven unsuccessful so far. Thus, the PM6 semiempirical molecular orbital method was employed to optimize the geometry of all hexagonal metallodendrimers **3a**–**c**. The optimized structure of each metallodendrimer featured a very similar, roughly planar hexagonal ring at the core surrounded by the dendron subunits at corners (Figures 3 and S7). Moreover, the size of the hexagonal metallodendrimers was determined as well. For instance, in the case of **3c**, the hexagonal ring-shaped metallodendrimer had an internal radius of ~1.4 nm, while the outer radius averaged 3.4 nm.

Fabrication of Vesicle-Like Nanostructures Based on Hierarchical Self-Assembly of Metallodendrimers. The existence of multiple intermolecular interactions (e.g., π–π stacking, CH–π interactions, and hydrogen bonds) imposed by peripherally DMIP-functionalized poly(benzyl ether) dendrons in hexagonal metallodendrimers **3a**–**c** stimulated us to investigate their hierarchical self-assembly behaviors in various solvents by employing scanning electron microscopy (SEM).

dx.doi.org/10.1021/ja500152a | J. Am. Chem. Soc. 2014, 136, 5993–6001

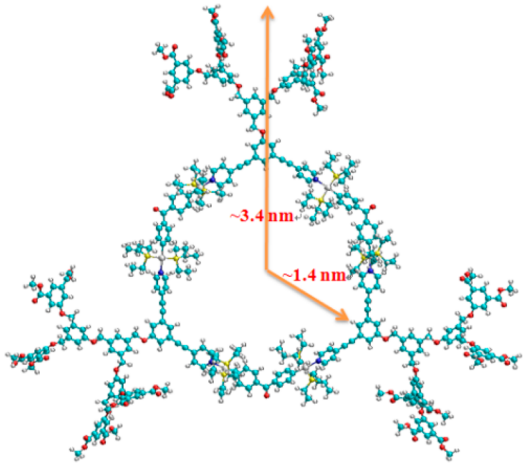

Figure 3. Geometrical structure of **3c** optimized by the PM6 semiempirical molecular orbital method.

SEM samples were prepared by depositing the solution of metallacycles onto a SiO_2/Si substrate followed by a slow evaporation in air at room temperature. As demonstrated in Figures 4a and S8, the [G-2] dendritic hexagon **3c** exhibited

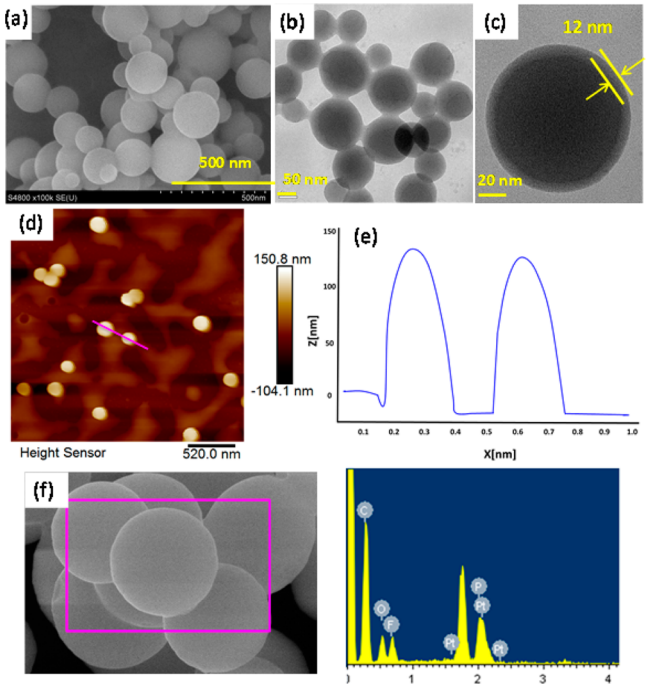

Figure 4. SEM images of **3c** (a, the scale bar is 500 nm); TEM images of **3c** (b, the scale bar is 50 nm); the enlarged TEM image (c, the scale bar is 20 nm); AFM image of **3c** (d); height profile of the assemblies along the pink line in d (e); and the EDX results (f, right) of **3c** collected from the area marked by the pink boxes (f, left).

spherical morphology with a diameter of ca. 150 nm in the mixed solvents of acetone and tetrahydrofuran (THF) (v/v, 4/1). In contrast, the analogous assemblies **3a** and **3b** displayed relatively irregular morphologies in the same condition (Figures S9 and S10). This result indicated that the dendron generation influenced the hierarchical self-assembly behavior. The second generation poly(benzyl ether) dendrimers turned out to be the best self-association moiety, as indicated in the previous reports.[16] Therefore, the second generation metalladendrimer **3c** was selected as a representative to study the hierarchical self-assembly behavior in detail.

In order to obtain the additional information about the nature of the assembled nanostructures, transmission electron microscopy (TEM) measurements were performed. A solution of **3c** was deposited on copper grids, followed by a slow evaporation in air at room temperature. The existence of the spherical entities with a diameter of ~150 nm was observed (Figures 4b and S11), which was in good agreement with SEM measurements. It was found that the spherical structures showed a clear contrast between the interior and periphery, which is consistent with the typical characteristic of vesicular structures. The thickness of the vesicle-like structure was calculated to be ~12 nm from their TEM images (Figure 4c). Considering that the extended length of **3c** calculated by PM6 semiempirical molecular orbital method was around 6.0 nm (Figure 3), the vesicle-like structures might possess a bilayer structure as shown in Figure 8c. The further morphology investigation of the obtained nanostructures from [G-2] hexagonal metallodendrimer **3c** by using atomic force microscope (AFM) was carried out. The similar spherical structures (Figures 4d and S12) were found in AFM images, which was consistent with the discovery in SEM and TEM studies. Moreover, the investigation of energy dispersive X-ray spectroscope (EDX) was carried out to gain the further insight into the elemental composition of these nanostructures. Elemental composition of carbon, oxygen, fluorine, platinum, and phosphorus were found from the spherical aggregates (Figure 4f), which strongly supported that these spherical nanostructures were entirely generated from the hierarchical self-assembly of hexagonal metallodendrimer **3c**.

A further spectroscopic investigation of metallodendrimer in solution was carried out to gain more insight into the aggregation mode during the formation of vesicle-like structures. The aggregation behavior of **3c** was studied by using UV−vis spectroscopy. The intensity of the broad absorption of **3c** significantly decreased when the solution of **3c** (6.67×10^{-5} M) was prepared in the mixed solvents of acetone and THF compared with that in dichloromethane (Figure S13). This decrease might be caused by the formation of aggregates in the mixed solvents of acetone and THF, which reduced the number of absorbing species in such solution.[17] Additionally, the same solution of **3c** (6.67×10^{-5} M) showed the clear evidence of Tyndall effect (Figures 5 and S13), demonstrating the existence of nanoscale aggregates. Notably, this scattering phenomenon did not occur for the solution of

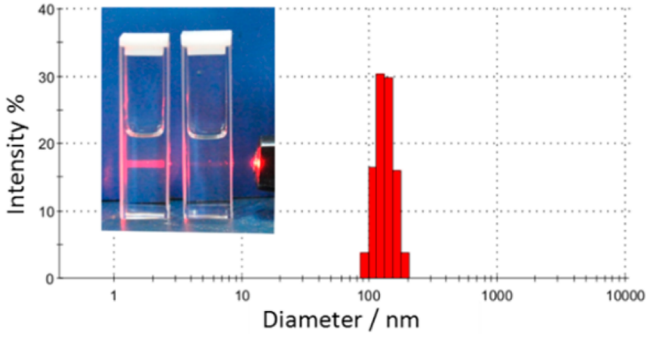

Figure 5. DLS data at a scattering angle of 90°for the self-assembled vesicles generated from **3c** with an inset showing Tyndall effect of hexagon **3c** (left) and ligand **1c** (right).

dx.doi.org/10.1021/ja500152a | J. Am. Chem. Soc. 2014, 136, 5993−6001

the free ligand **1c** even at the higher concentration (2.00×10^{-4} M), which supported that the hexagonal core was required for the formation of aggregates. Furthermore, the plots of optical transmittance versus concentration at 350 nm displayed two regimes, which revealed the critical aggregation concentrations (CACs) to be ca. 9.0×10^{-6} M for **3c** (Figure S14).

With the aim to obtaining the more structural information on the assembly of **3c**, particularly the size distribution of its aggregates, concentration-dependent (CD) dynamic light scattering (DLS) experiments were performed. Evidently, it was observed that hexagonal metallodendrimer **3c** formed the particles of 100−200 nm diameter with the distribution centered at 155 nm in the mixed solvents of acetone and THF (2.0×10^{-4} M) (Figures 5 and S15), which was in good agreement with the SEM and TEM results. In addition, the value of radius was found to increase when the concentration exceeded the CACs, which was in good agreement with the UV results (Figure S16).

CD and temperature-dependent (TD) ^{1}H NMR spectra of **3c** were recorded to gain the driving forces for the formation of such regular aggregates. In the CD-^{1}H NMR experiments of **3c** in the mixed solvents of acetone-d_6 and THF-d_8 (v/v: 4/1), the increase of concentration (from 1.00×10^{-5} to 3.25×10^{-3} M) resulted in the slight upfield shifts of the resonance signals for the aromatic protons on the peripheral DMIP rings and the internal benzyl rings (Figure S17). Regarding the TD-^{1}H NMR experiments, these resonance signals were found to be gradually shifted downfield when the temperature increased from 278 to 328 K (Figure S18). Notably, the signals corresponding to the benzyl ring at the focal point remained unchanged. Based on all above experimental results, we presumed that the formation of such regular nanostructures might be mainly driven by the $\pi-\pi$ stacking and CH$-\pi$ interactions of the periphery dendrons.

Stimuli-Responsive Properties of Vesicle-Like Nanostructures. The dynamic nature of metal−ligand bonds inspired us to further investigate the stimuli-responsive property of such hierarchical self-assembled vesicles from hexagonal metallodendrimers **3c**. It was found that with the addition of 6 equiv of tetrabutylammonium bromide (Bu_4NBr) into the vesicular solution of **3c**, the vesicle-like structures generated from **3c** on the basis of hierarchical self-assembly were totally destroyed and transformed into micelles. As shown in Figure 6, both the SEM and TEM images confirmed the formation of micelles after the addition of Bu_4NBr. Moreover, such stimuli-responsive property was further verified by DLS experiments. After the addition of Bu_4NBr, the diameter of the aggregates formed from **3c** was found to decrease from ∼150 to ∼15 nm (Figure 6c), which was consistent with the corresponding SEM and TEM images as displayed in Figure 6a,b. These DLS experimental results revealed the transformation from the regular vesicles to the micellar structure, thus providing the convincing proof to support the stimuli-responsive phenomena.

We assumed that such stimuli-responsive morphology transition was essentially as a consequence of the halide-induced disassembly of the hexagonal metallacycle (Scheme S2). In order to provide the further support for the stimuli-responsive disassembly and reassembly process, *in situ* multinuclear NMR (^{1}H and ^{31}P) investigation of **3c** in CD_2Cl_2 was carried out. As expected, the addition and removal of bromide anion caused the disassembly and reassembly of the hexagonal core as detected in multinuclear NMR (^{1}H and ^{31}P) investigation. For example, the typical proton signals of

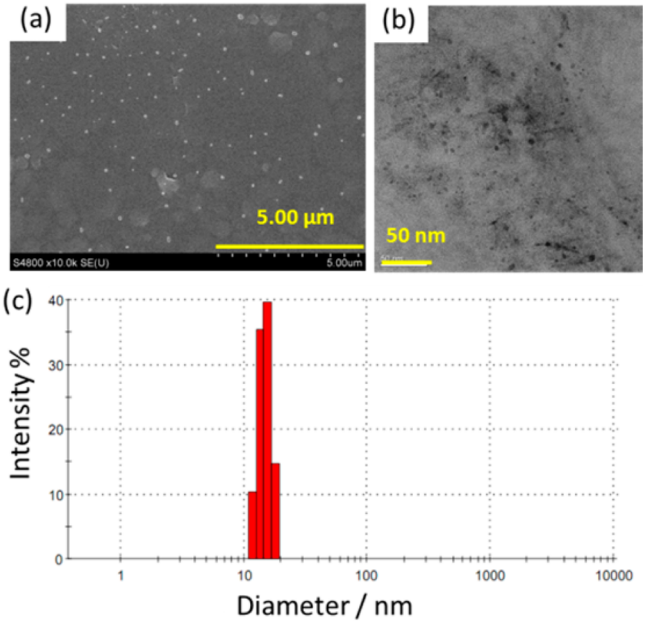

Figure 6. SEM images (a, the scale bar is 5 μm), TEM images (b, the scale bar is 50 nm) and DLS data (c) of **3c** after the addition of 6 equiv of Bu_4NBr to the sample of **3c** in acetone/THF = 4/1 (0.2 mM).

hexagonal metallacycles disappeared, and the resonance from free ligand **1c** and new Pt−Br complex **4** in a 1:1 ratio appeared in the ^{1}H NMR spectrum after the addition of Bu_4NBr to the solution of **3c** in CD_2Cl_2 (Figures S22 and S23). Moreover, upon adding $AgPF_6$ to the mixture, the original signals in the ^{1}H and ^{31}P NMR spectra were restored (Figures S22 and S23). Such NMR changes provided the direct evidence for the stimuli-responsive quantitative disassembly and reassembly of the supramolecular hexagonal metallodendrimers.

Encapsulation and Controlled Release. Supramolecular self-assembled nanostructures processing stimuli-responsive properties have attracted considerable interest because of their promising applications such as biosensors, catalysis, drug delivery and so on.[18] The stimuli-responsive properties of the self-assembled vesicle-like structures can be used for encapsulation and the triggered release of active substances (e.g., drugs, fragrances, and flavor additives). Thus, we envisioned that this kind of stimuli-responsive vesicles might be employed to encapsulate and release small molecules. Thus, 8-(4-hydroxypenyl)-4,4-difluoro-1,3,5,7-tetramethyl-4-bora-3a,4a-diaza-*s*-indacene (BODIPY) and sulforhodamine B (SRB) were selected as model guests, from which the fluorescent dye-loaded colloids were prepared to perform the controlled release experiments.

To prepare the dye-loaded vesicles, fluorescent dye BODIPY or SRB was quickly added into a freshly prepared vesicular solution, respectively. After standing overnight, the unloaded fluorescent molecules were removed by dialysis. After removing the unloaded dye molecules, the BODIPY-loaded vesicular solution turned to light-green, while the SRB-loaded vesicular solution became light-red compared with the pale-yellow unloaded vesicular solution, demonstrating that the dye molecules were successfully encapsulated into the vesicle-like structures. Moreover, in the emission spectra of dye-loaded vesicular solution, as shown in Figure S26, almost no fluorescent signals, corresponding to the characteristic emission of SRB or BODIPY, were observed, indicating that SRB or

dx.doi.org/10.1021/ja500152a | J. Am. Chem. Soc. 2014, 136, 5993−6001

BODIPY molecules were stably located in the vesicles. Furthermore, as displayed in Figure 7a,c, SEM images showed

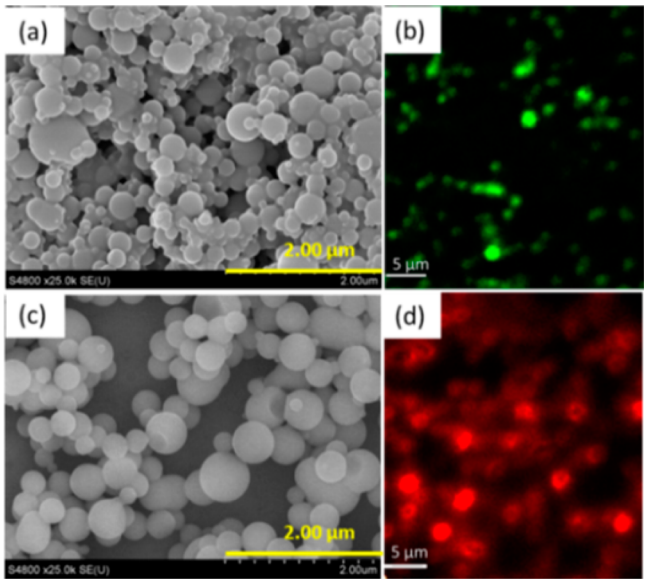

Figure 7. SEM and LSCM images of vesicle **3c** containing the entrapped BODIPY (a, b) and SRB (c, d).

that these dye-loaded vesicles were much larger in size (averaged diameter of 240 nm for BODIPY-loaded vesicles, Figure 7a; 300 nm for SRB-loaded vesicles, Figure 7c) than that of the original unloaded vesicles (average diameter of 150 nm), which was consistent with the size increase of vesicles after encapsulation of guests reported previously.[19] More intuitively, the green or red luminescence was emitted from the nanoscale structures after loading the fluorescent dye BODIPY or SRB, respectively, which was directly observed by laser scanning confocal microscope (LSCM) images as exhibited in Figure 7b,d (Figures S24 and S25). These results clearly showed that the vesicle-like nanostructures were filled with fluorescence dye in solution.

The controlled release of dye molecules was monitored through the increasing fluorescence of the solution outside the dialysis tube. With the addition of Bu_4NBr, the release of fluorescent dyes from the inside of vesicles was achieved accompanied by an increasing intensity in the fluorescence emission spectra (Figure 8a). From the curve in Figure 8b, a release of SRB was observed upon addition of Bu_4NBr. While in contrast, in the absence of external stimuli, the capsules only showed a low-level release. Similar phenomenon was observed in the controlled release experiment of the BODIPY-loaded vesicles (Figure S27). This phenomenon can be explained by a halide-triggered vesicles−micelles transition. The addition of Bu_4NBr resulted in the collapse of the vesicles into micelles with a concomitant release of the encapsulated fluorescence dyes (Figure 8c). Thus, these hierarchically self-assembled vesicle-like structures can serve as nanocapsules that are able to encapsulate and release functional molecules over a tunable time and quantity through the artificial control.

CONCLUSIONS

In summary, a series of hexagonal metallodendrimers **3a−c** were successfully prepared with high efficiency through coordination-driven self-assembly. It was found that the second generation metallodendrimer **3c** was able to self-assemble into the vesicle-like structures mainly driven by the $\pi-\pi$ stacking, CH$-\pi$ interactions, and hydrogen bonds imposed by the periphery dendrons. The obtained vesicles were monodisperse in shape and relatively monodisperse in size as detected in SEM, TEM, AFM, and DLS measurement. Notably, due to the dynamic nature of metal−ligand bonds, the disassembly and reassembly of the obtained hexagonal metallodendrimers could be reversibly controlled by the addition and removal of bromide ions, resulting in the transition between the vesicles and micelles. This phenomenon can be utilized for the controlled release of encapsulated guest molecules. By taking

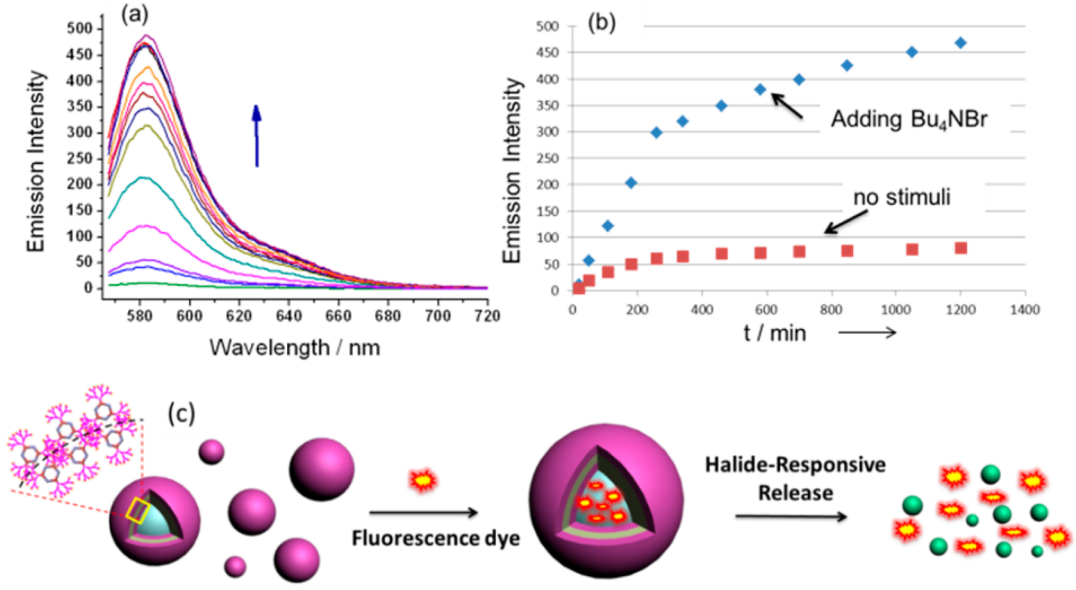

Figure 8. (a) The emission change of the solution outside the dialysis tube after adding 6 equiv of Bu_4NBr into dialysis tube (λ_{ex}= 550 nm) with different time. (b) The intensity change in emission of SRB at 583 nm after the addition of Bu_4NBr and in comparison with the free release of SRB from the vesicular solution without stimuli. (c) The illustration of the process of halide-responsive release of fluorescent molecules.

dx.doi.org/10.1021/ja500152a | J. Am. Chem. Soc. 2014, 136, 5993−6001

the advantage of the halide-induced vesicles−micelles transition, the controlled release of fluorescence dyes was successfully realized. Since the size and shape of the cavities in metallodendrimers could be fine-turned by the proper choice of dendritic building blocks and complementary precursors with the predefined angles and symmetry, it is possible to manipulate the resulted nanostructure by modulating space orientation of peripheral dendrons. Moreover, considering the fact that the stimuli conditions are readily realized, it is anticipated that this kind of stimuli-responsive smart nanostructures have the potential as nanocapsules for guest capsulation and controlled release. Thus, this proof-of-principle study provided a new avenue to the construction of novel "smart" materials containing well-defined metallacycles as scaffold via hierarchical self-assembly, which have the potential applications in functional molecules delivery and release.

EXPERIMENTAL SECTION

Full experimental details are provided in the Supporting Information. The most important information is summarized briefly below.

General Procedure for Preparation of Supramolecular Hexagonal Metallodendrimers. Hexagonal metallodendrimers **3a−c** were synthesized according to the synthetic routes shown in Scheme 1. All reagents were purchased from commercial suppliers and used without further purification. Ligands **1a−c** were prepared according to literature procedures. Nuclear magnetic resonance (NMR) spectra were recorded on Bruker 400 MHz spectrometer, with working frequencies of 400 MHz for ^{1}H and 161.9 MHz for ^{31}P nuclei, respectively. Chemical shifts are reported in parts per million relative to the signals corresponding to the residual nondeuterated solvent (CD_2Cl_2: δ = 5.32 ppm), and ^{31}P NMR resonances are referenced to an internal standard sample of 85% H_3PO_4 (δ 0.0). The CSI-TOF-MS spectra were acquired using an AccuTOF CS mass spectrometer (JMS-T100CS, JEOL, Tokyo, Japan).

*Synthesis of **3a**.* The dipyridyl donor ligand **1a** (9.9 mg, 19.7 μmol) and the organoplatinum 120° acceptor **2** (22.9 mg, 19.6 μmol) were weighed accurately into a glass vial. To the vial was added 2 mL of CH_2Cl_2 solvent, and the reaction solution was then stirred at room temperature for 10 h to yield a homogeneous orange solution. Then acetone (3 mL) was added, followed by the addition of a saturated aqueous solution of KPF_6 into the bottle with continuous stirring (10 min) to precipitate the product. The reaction mixture was centrifuged, washed several times with water, and dried. The pale-yellow product **3a** (32.2 mg, 98%) was collected and redissolved in CD_2Cl_2 for NMR analysis. IR (neat): ν/cm^{-1} 3041, 2951, 2852, 2215, 1725, 1608, 1576, 1418, 1247, 1207, 1176, 1065, 1033, 1004, 925, 837, 734. ^{1}H NMR (CD_2Cl_2, 400 MHz): δ 8.67 (d, J = 5.6 Hz, 12H, H_α-Py), 8.64 (s, 3H, PhH), 8.35 (s, 6H, PhH), 7.81 (d, J = 5.6 Hz, 12H, H_β-Py), 7.62 (s, 3H, PhH), 7.56−7.51 (m, 24H, ArH), 7.37 (s, 6H, PhH), 5.26 (s, 6H), 3.95 (s, 18H), 1.35 (s, 72H), 1.18−1.11 (m, 108H). ^{31}P{^{1}H} NMR (CD_2Cl_2, 161.9 MHz): δ 13.6 (s, $^{1}J_{Pt-P}$ = 2650.3 Hz). ^{13}C NMR (CD_2Cl_2, 100 MHz): δ 7.77, 12.57, 12.74, 12.91, 52.78, 69.76, 86.29, 97.60, 120.39, 123.39, 125.84, 129.91, 130.54, 131.61, 132.80, 133.77, 135.02, 136.15, 137.71, 141.47, 151.97, 158.79, 166.20, 196.55. ESI-MS: m/z: 772.18 $[M-6PF_6^-]^{6+}$, 955.58 $[M-5PF_6^-]^{5+}$, 1230.69 $[M-4PF_6^-]^{4+}$, 1689.21 $[M-3PF_6^-]^{3+}$. Anal. calcd for $C_{204}H_{270}F_{36}N_6O_{18}P_{18}Pt_6$: C, 44.50; H, 4.94; N, 1.53. Found: C, 44.24; H, 5.05; N, 1.64.

*Synthesis of **3b**.* Following the procedure for **3a**, **1b** (14.9 mg, 17.93 μmol) and the organoplatinum 120° acceptor **2** (20.9 mg, 17.91 μmol) yielded **3b** as a pale-yellow solid (33.9 mg, 95%). IR (neat): ν/cm^{-1} 3046, 2951, 2924, 2853, 2364, 2215, 1724, 1608, 1577, 1457, 1433, 1338, 1244, 1207, 1117, 1066, 1032, 1004, 926, 839, 758. ^{1}H NMR (CD_2Cl_2, 400 MHz): δ 8.68 (d, J = 5.2 Hz, 12H, H_α-Py), 8.26 (s, 6H, ArH), 7.85 (s, 12H, ArH), 7.81 (d, J = 6.0 Hz, 12H, H_β-Py), 7.61−7.51 (m, 36H, ArH), 7.35 (s, 6H, PhH), 5.24 (s, 12H), 5.22 (s, 6H), 3.92 (s, 36H), 1.36−1.35 (s, 72H), 1.18−1.12 (m, 108H). ^{31}P{^{1}H} NMR (CD_2Cl_2, 161.9 MHz): δ 13.4 (s, $^{1}J_{Pt-P}$ = 2655.2 Hz). ^{13}C NMR (CD_2Cl_2, 100 MHz): δ 7.78, 12.62, 12.78, 12.95, 52.72, 70.40, 86.25, 97.73, 120.25, 123.34, 123.42, 126.66, 126.76, 129.92, 132.41, 133.80, 135.07, 136.18, 137.55, 137.80, 141.46, 151.99, 159.07, 166.25, 196.56. ESI-MS: m/z: 936.10 $[M-6PF_6^-]^{6+}$, 1152.31 $[M-5PF_6^-]^{5+}$, 1476.86 $[M-4PF_6]^{4+}$, 2017.05 $[M-3PF_6^-]^{3+}$. Anal. calcd for $C_{258}H_{318}F_{36}N_6O_{36}P_{18}Pt_6$: C, 47.74; H, 4.94; N, 1.29. Found: C, 47.66; H, 4.94; N, 1.50.

*Synthesis of **3c**.* Following the procedure for **3a**, **1c** (13.9 mg, 9.34 μmol) and the organoplatinum 120° acceptor **2** (10.9 mg, 9.34 μmol) yielded **3c** as a pale-yellow solid (22.5 mg, 91%). IR (neat): ν/cm^{-1} 3052, 2950, 2925, 2852, 2359, 2342, 2220, 1721, 1594, 1476, 1458, 1433, 1336, 1309, 1239, 1207, 1115, 1069, 1031, 1001, 925, 836, 757. ^{1}H NMR (CD_2Cl_2, 400 MHz): δ 8.67 (d, J = 5.2 Hz, 12H, H_α-Py), 8.23 (s, 12H, ArH), 7.81−7.79 (d, 36H, H_β-Py and ArH), 7.61−7.53 (m, 36H, ArH), 7.35 (s, 6H, PhH), 7.16 (s, 6H, ArH), 7.09 (s, 12H, ArH), 5.18−5.16 (d, 42H), 3.90 (s, 72H), 1.35−1.34 (m, 72H), 1.18−1.12 (m, 108H). ^{31}P{^{1}H} NMR (CD_2Cl_2, 161.9 MHz): δ 13.56 (s, $^{1}J_{Pt-P}$ = 2661.6 Hz). ^{13}C NMR (CD_2Cl_2, 100 MHz): δ 7.79, 12.80, 12.97, 13.08, 52.71, 68.95, 70.16, 70.42, 86.65, 97.70, 113.81, 119.22, 120.25, 123.36, 126.70, 128.99, 129,94, 132.38, 136.19, 137.36, 138.31, 138.84, 152.02, 159.08, 159.61, 166.24, 196.48. ESI-MS: m/z: 1264.47 $[M-6PF_6^-]^{6+}$, 1546.33 $[M-5PF_6^-]^{5+}$, 1969.10 $[M-4PF_6]^{4+}$. Anal. calcd for $C_{366}H_{414}F_{36}N_6O_{72}P_{18}Pt_6{\cdot}CH_2Cl_2$: C, 51.58; H, 4.91, N, 0.98. Found: C, 51.52; H, 5.18. N, 1.07.

SEM, TEM, EDX, AFM, and DLS Experiments. SEM images of complex **3a−c** were obtained using a S-4800 (Hitachi Ltd.) with an accelerating voltage of 3.0−10.0 kV. Samples were prepared by dropping solutions onto a silicon wafer. To minimize sample charging, a thin layer of Au was deposited onto the samples before SEM examination. TEM images were recorded on a Tecnai G^2 F30 (FEI Ltd.). The sample for TEM measurement was prepared by dropping the solution onto a carbon-coated copper grid. EDX measurements were performed using a S-4800 (Hitachi Ltd.) with an voltage of 10.0 kV. AFM images were obtained on a Dimension FastScan (Bruker) using ScanAsyst mode under the ambient condition. Scanasyst-Fluid$^+$ probes were used for scan. The AFM samples were prepared by dropping solutions onto a silicon wafer. DLS measurements were performed under a Malvern Zetasizer Nano-ZS light scattering apparatus (Malvern Instruments, U.K.) with a He−Ne laser (633 nm, 4 mW).

UV−vis Absorption and Fluorescence Emission Spectra. UV−vis spectra were recorded in a quartz cell (light path 10 mm) on a Cary 50Bio UV−vis spectrophotometer. Steady-state fluorescence spectra were recorded in a conventional quartz cell (light path 10 mm) on a Cary Eclipse fluorescence spectrophotometer.

Laser Scanning Confocal Microscopy Experiments. LSCM imaging was performed with an OLYMPUS ZX81 laser

dx.doi.org/10.1021/ja500152a | J. Am. Chem. Soc. 2014, 136, 5993−6001

scanning microscopy and a 60× oil-immersion objective lens. 470 nm laser (for BODIPY loaded nanostructures) or 550 nm laser (for LRB loaded nanostructures) was selected as the excitation source, respectively.

■ ASSOCIATED CONTENT

Supporting Information

Synthesis, characterization, and other experimental details. This materials is available free of charge via the Internet at http://pubs.acs.org.

■ AUTHOR INFORMATION

Corresponding Author

hbyang@chem.ecnu.edu.cn

Notes

The authors declare no competing financial interest.

■ ACKNOWLEDGMENTS

This work was financially supported by NSFC/China (nos. 21322206 and 21132005), the Key Basic Research Project of Shanghai Science and Technology Commission (no. 13JC1402200), Fok Ying Tung Education Foundation (no. 131014), and the Program for Changjiang Scholars and Innovative Research Team in University. We thank Prof. Minghua Liu and Dr. Li Zhang at ICCAS for their help with AFM measuremts.

■ REFERENCES

(1) (a) Newkome, G. R.; Moorefield, C. N.; Vögtle, F. *Dendrimers and Dendrons: Concepts, Syntheses, Applications*; Wiley-VCH: New York, 2001;. (b) Moorefield, C. N.; Perera, S.; Newkome, G. R. *Dendrimer Chemistry: Supramolecular Perspectives and Applications*; John Wiley & Sons: New York, 2012;. (c) Zeng, F.; Zimmerman, S. C. *Chem. Rev.* **1997**, *97*, 1681−1712. (d) Bosman, A. W.; Janssen, H. M.; Meijer, E. W. *Chem. Rev.* **1999**, *99*, 1665−1688. (e) Crespo, L.; Sanclimens, G.; Pons, M.; Giralt, E.; Royo, M.; Albericio, F. *Chem. Rev.* **2005**, *105*, 1663−1681.

(2) (a) Hecht, S.; Fréchet, J. M. J. *Angew. Chem., Int. Ed.* **2001**, *40*, 74−91. (b) Lee, C. C.; MacKay, J. A.; Fréchet, J. M. J.; Szoka, F. C. *Nat. Biotechnol.* **2005**, *23*, 1517−1526. (c) Crooks, R. M.; Zhao, M.; Sun, L.; Chechik, V.; Yeung, L. K. *Acc. Chem. Res.* **2001**, *34*, 181−190. (d) Cheng, Y.; Zhao, L.; Li, Y.; Xu, T. *Chem. Soc. Rev.* **2011**, *40*, 2673−2703. (e) Svenson, S.; Tomalia, D. *Adv. Drug Delivery Rev.* **2005**, *57*, 2106−2129. (f) Baars, M. W. P. L.; Meijer, E. W. *Top. Curr. Chem.* **2000**, *210*, 131−182. (g) Puntoriero, F.; Ceroni, P.; Balzani, V.; Bergamini, G.; Vögtle, F. *J. Am. Chem. Soc.* **2007**, *129*, 10714−10719. (h) Cheng, Y. Y.; Zhao, L. B.; Li, Y. W.; Xu, T. W. *Chem. Soc. Rev.* **2011**, *40*, 2673−2703. (i) Hu, J. J.; Xu, T. W.; Cheng, Y. Y. *Chem. Rev.* **2012**, *112*, 3856−3891. (j) Wang, X. Y.; Cai, X. P.; Hu, J. J.; Shao, N. M.; Wang, F.; Zhang, Q.; Xiao, J.; Cheng, Y. Y. *J. Am. Chem. Soc.* **2013**, *135*, 9805−9810. (k) Liu, H. M.; Wang, H.; Yang, W. J.; Cheng, Y. Y. *J. Am. Chem. Soc.* **2012**, *134*, 17680−17687.

(3) (a) Astruc, D.; Boisselier, E.; Ornelas, C. *Chem. Rev.* **2010**, *110*, 1857−1959. (b) Peterca, M.; Imam, M. R.; Ahn, C. H.; Balagurusamy, V. S.; Wilson, D. A.; Rosen, B. M.; Percec, V. *J. Am. Chem. Soc.* **2011**, *133*, 2311−2328. (c) Narayanan, V. V.; Newkome, G. R. *Top. Curr. Chem.* **1998**, *197*, 19−77. (d) Smith, D. K.; Diederich, F. *Top. Curr. Chem.* **2000**, *210*, 183−227. (e) Zimmerman, S. C.; Lawless, L. J. *Top. Curr. Chem.* **2001**, *217*, 95−120. (f) Emrick, T.; Fréchet, J. M. J. *Curr. Opin. Colloid Interface Sci.* **1999**, *4*, 15−23. (g) Zeng, F. W.; Zimmerman, S. C. *Chem. Rev.* **1997**, *97*, 1681−1712.

(4) (a) Newkome, G. R.; Moorefield, C. N.; Baker, G. R.; Johnson, A. L.; Behera, R. K. *Angew. Chem., Int. Ed. Engl.* **1991**, *30*, 1176−1178. (b) Newkome, G. R.; Cardullo, F.; Constable, E. C.; Moorefield, C. N.; Thompson, A. M. W. C. *J. Chem. Soc., Chem. Commun.* **1993**, 925−927.

(5) (a) Denti, G.; Serroni, S.; Campagna, S.; Ricevuto, V.; Balzani, V. *Inorg. Chim. Acta* **1991**, *182*, 127−129. (b) Denti, G.; Campagna, S.; Serroni, S.; Ciano, M.; Balzani, V. *J. Am. Chem. Soc.* **1992**, *114*, 2944−2982. (c) Campagna, S.; Denti, G.; Serroni, S.; Ciano, M.; Juris, A.; Balzani, V. *Inorg. Chem.* **1992**, *31*, 2982−2984.

(6) (a) Gorman, C. *Adv. Mater.* **1998**, *10*, 295−309. (b) Onitsuka, K.; Takahashi, S. *Top. Curr. Chem.* **2003**, *228*, 39−63. (c) Hwang, S.-H.; Shreiner, C. D.; Moorefield, C. N.; Newkome, G. R. *New J. Chem.* **2007**, *31*, 1192−1217. (d) Serroni, S.; Campagna, S.; Puntoriero, F.; Pietro, C. D.; McClenaghan, N. D.; Loiseau, F. *Chem. Soc. Rev.* **2001**, *30*, 367−375. (e) Astruc, D.; Ornelas, C.; Ruiz, J. *Acc. Chem. Res.* **2008**, *41*, 841−856.

(7) (a) Wang, Y.; Lin, H.-X.; Chen, L.; Ding, S.-Y.; Lei, Z.-C.; Li, D.-Y.; Cao, X.-Y.; Liang, H.-J.; Jiang, Y.-B.; Tian, Z.-Q. *Chem. Soc. Rev.* **2014**, *43*, 399−411. (b) Kumar, D. K.; Steed, J. W. *Chem. Soc. Rev.*, 2014, *43*, DOI: 10.1039/C3CS60224;. (c) Han, M.; Michel, R.; He, B.; Chen, Y.-S.; Stalke, D.; John, M.; Clever, G. H. *Angew. Chem.* **2013**, *125*, 1358−1362; *Angew. Chem., Int. Ed.* **2013**, *52*, 1319−1323. (d) Clever, A. H.; Shionoya, M. *Coord. Chem. Rev.* **2010**, *254*, 2391−2402. (e) Takezawa, Y.; Shionoya, M. *Acc. Chem. Res.* **2012**, *45*, 2066−2076. (f) Yoshizawa, M.; Klosterman J. K. *Chem. Soc. Rev.*, 2013, *42*, DOI:10.1039/C3CS60315F;. (g) Dsouza, R. N.; Pischel, U.; Nau, W. M. *Chem. Rev.* **2011**, *111*, 7941−7980. (h) Duttwyler, S.; Zhang, Y.; Linden, A.; Reed, C. A.; Baldridge, K. K.; S. Siegel, J. *Angew. Chem., Int. Ed.* **2009**, *48*, 3787−3790. (i) Luca, G. De; Liscio, A.; Maccagnani, P.; Nolde, F.; Palermo, V.; Müllen, K.; Samorì, P. *Adv. Funct. Mater.* **2007**, *17*, 3791−3798.

(8) (a) Lu, Y.; Liu, J. *Acc. Chem. Res.* **2007**, *40*, 315−323. (b) Ganta, S.; Devalapally, H.; Shahiwala, A.; Amiji, M. *J. Cont. Rel.* **2008**, *126*, 187−204. (c) Cotí, K. K.; Belowich, M. E.; Liong, M.; Ambrogio, M. W.; Lau, Y. A.; Khatib, H. A.; Zink, J. I.; Khashab, N. M.; Stoddart, J. F. *Nanoscale* **2009**, *1*, 16−39. (d) Rybtchinski, B. *ACS Nano* **2011**, *5*, 6791−6818. (e) Mura, S.; Nicolas, J.; Couvreur, P. *Nat. mat.* **2013**, *12*, 991−1003.

(9) For selected examples, see: (a) Newkome, G. R.; Baker, G. R.; Saunders, M. J.; Russo, P. S.; Gupta, V. K.; Yao, Z. Q.; Miller, J. E.; Bouillion, K. *J. Chem. Soc. Chem. Commun.* **1986**, 752−753. (b) Marmillon, C.; Gauffre, F.; Gulik-Krzywicki, T.; Loup, C.; Caminade, A. M.; Majoral, J. P.; Vors, J. P.; Rump, E. *Angew. Chem., Int. Ed.* **2001**, *40*, 2626−2629. (c) Jang, W. D.; Jiang, D. L.; Aida, T. *J. Am. Chem. Soc.* **2000**, *122*, 3232−3233. (d) Kim, C.; Kim, K. T.; Chang, Y.; Song, H. H.; Cho, T. Y.; Jeon, H. J. *J. Am. Chem. Soc.* **2001**, *123*, 5586−5587. (e) Hirst, A. R.; Smith, D. K.; Feiters, M. C.; Geurts, H. P. M.; Wright, A. C. *J. Am. Chem. Soc.* **2003**, *125*, 9010−9011. (f) Zubarev, E. R.; Pralle, M. U.; Sone, E. D.; Stupp, S. I. *J. Am. Chem. Soc.* **2001**, *123*, 4105−4106. (g) Yoshida, M.; Fresco, Z. M.; Ohnishi, S.; Fréchet, J. M. J. *Macromolecules* **2005**, *38*, 334−344. (h) Duan, P. F.; Liu, M. H. *Langmuir* **2009**, *25*, 8706−8713. (i) Wang, Q. G.; Mynar, J. L.; Yoshida, M.; Lee, E.; Lee, M.; Okuro, K.; Kinbara, K.; Aida, T. *Nature* **2010**, *463*, 339−343. (j) Kuang, G. C.; Jia, X. R.; Teng, M. J.; Chen, E. Q.; Li, W. S.; Ji, Y. *Chem. Mater.* **2012**, *24*, 71−80.

(10) (a) Chan, Y.; Moorefield, C. N.; Soler, M.; Newkome, G. R. *Chem.—Eur. J.* **2010**, *16*, 1768−1771. (b) Baytekin, H. T.; Sahre, M.; Rang, A.; Engeser, M.; Schulz, A.; Schalley, C. A. *Small* **2008**, *4*, 1823−1834. (c) Yan, X.; Jiang, B.; Cook, T. R.; Zhang, Y.; Li, J.; Yu, Y.; Huang, F.; Yang, H.-B.; Stang, P. J. *J. Am. Chem. Soc.* **2013**, *135*, 16813−16816.

(11) (a) Cook, T. R.; Zheng, Y.-R.; Stang, P. J. *Chem. Rev.* **2013**, *113*, 734−777. (b) Leininger, S.; Olenyuk, B.; Stang, P. J. *Chem. Rev.* **2000**, *100*, 853−907. (c) Fujita, M.; Tominaga, M.; Hori, A.; Therrien, B. *Acc. Chem. Res.* **2005**, *38*, 369−378. (d) Spokoyny, A. M.; Kim, D.; Sumrein, A.; Mirkin, C. A. *Chem. Soc. Rev.* **2009**, *38*, 1218−1227. (e) Pluth, M. D.; Raymond, K. N. *Chem. Soc. Rev.* **2007**, *36*, 161−171. (f) Liu, S.; Han, Y.-F.; Jin, G.-X. *Chem. Soc. Rev.* **2007**, *36*, 1543−1560. (g) Newkome, G. R.; Shreiner, C. *Chem. Rev.* **2010**, *110*, 6338−6442. (h) Chakrabarty, R.; Mukherjee, P. S.; Stang, P. J. *Chem. Rev.* **2011**, *111*, 6810−6918.

(12) (a) Leininger, S.; Schmitz, M.; Stang, P. J. *Org. Lett.* **1999**, *1*, 1921−1923. (b) Clever, G. H.; Kawamura, W.; Tashiro, S.; Shiro, M.;

Shionoya, M. *Angew. Chem., Int. Ed.* **2012**, *51*, 2602−2609. (c) Wang, P.; Moorefield, C. N.; Newkome, G. R. *Angew. Chem., Int. Ed.* **2005**, *44*, 1679−1683. (d) Harano, K.; Hiraoka, S.; Shionoya, M. *J. Am. Chem. Soc.* **2007**, *129*, 5300−5301. (e) Lusby, P. J.; Müller, P.; Pike, S. J.; Slawin, A. M. Z. *J. Am. Chem. Soc.* **2009**, *131*, 16398−16400. (f) Zhao, L.; Northrop, B. H.; Stang, P. J. *J. Am. Chem. Soc.* **2008**, *130*, 11886−11888. (g) Brown, A. M.; Ovchinnikov, M. V.; Stern, C. L.; Mirkin, C. A. *J. Am. Chem. Soc.* **2004**, *126*, 14316−14137.

(13) (a) Forgan, R. S.; Sauvage, J. P.; Stoddart, J. F. *Chem. Rev.* **2011**, *111*, 5434−5464. (b) Lee, S. J.; Hupp, J. T. *Coord. Chem. Rev.* **2006**, *250*, 1710−1723. (c) Pluth, M. D.; Bergman, R. G.; Raymond, K. N. *Acc. Chem. Res.* **2009**, *42*, 1650−1659. (d) Sumida, K.; Rogow, D. L.; Mason, J. A.; McDonald, T. M.; Bloch, E. D.; Herm, Z. R.; Bae, T. H.; Long, J. R. *Chem. Rev.* **2011**, *112*, 724−781. (e) Northrop, B. H.; Yang, H.-B.; Stang, P. J. *Chem. Commun.* **2008**, 5896−5908.

(14) (a) Chen, S.; Chen, L.-J.; Yang, H.-B.; Tian, H.; Zhu, W. *J. Am. Chem. Soc.* **2012**, *134*, 13596−13599. (b) Chen, L.-J.; Li, Q.-J.; He, J.; Tan, H.; Abliz, Z.; Yang, H.-B. *J. Org. Chem.* **2012**, *77*, 1148−1153. (c) Heo, J.; Mirkin, C. A. *Angew. Chem., Int. Ed.* **2006**, *45*, 941−944. (d) Barry, N. P. E.; Furrer, J.; Freudenreich, J.; Süss-Fink, G.; Therrien, B. *Eur. J. Inorg. Chem.* **2010**, 725−728. (e) Meng, W.; Clegg, J. K.; Thoburn, J. D.; Nitschke, J. R. *J. Am. Chem. Soc.* **2011**, *133*, 13652−13660. (f) Nakabayashi, K.; Kawano, M.; Yoshizawa, M.; Ohkoshi, S.; Fujita, M. *J. Am. Chem. Soc.* **2004**, *126*, 16694−16695. (g) Dong, V. M.; Fiedler, D.; Carl, B.; Bergman, R. G.; Raymond, K. N. *J. Am. Chem. Soc.* **2006**, *128*, 14464−14465.

(15) (a) Xu, L.; Chen, L.-J.; Yang, H.-B. *Chem. Commun.* 2013, DOI:10.1039/C3CC47484D;. (b) Yang, H.-B.; Hawkridge, A. M.; Huang, S. D.; Das, N.; Muddiman, D. C.; Stang, P. J. *J. Am. Chem. Soc.* **2007**, *129*, 2120−2129. (c) Yang, H.-B.; Das, N.; Huang, F.; Hawkridge, A. M.; Muddiman, D. C.; Stang, P. J. *J. Am. Chem. Soc.* **2006**, *128*, 10014−10015. (d) Yang, H.-B.; Northrop, B. H.; Zheng, Y.-R.; Ghosh, K.; Stang, P. J. *J. Org. Chem.* **2009**, *74*, 7067−7074. (e) Han, Q.; Li, Q.-J.; Wang, L.-L.; He, J.; Tan, H.; Abliz, Z.; Wang, C.-H.; Yang, H.-B. *J. Org. Chem.* **2011**, *76*, 9660−9669. (f) Xu, X.-D.; Ou-Yang, J.-K.; Zhang, J.; Zhang, Y.-Y.; Gong, H.; Yu, Y.-H.; Yang, H.-B. *Tetrahedron* **2013**, *69*, 1086−1091. (g) Zhao, G.-Z.; Li, Q.-J.; Chen, L.-J.; Tan, H.; Wang, C.-H.; Wang, D.-X.; Yang, H.-B. *Organometallics* **2011**, *30*, 5141−5146. (h) Han, Q.; Wang, L.-L.; Li, Q.-J.; Zhao, G.-Z.; He, J.; Hu, B.; Tan, H.; Abliz, Z.; Yu, Y.; Yang, H.-B. *J. Org. Chem.* **2012**, *77*, 3426−3432.

(16) (a) Feng, Y.; Liu, Z.-T.; Liu, J.; He, Y.-M.; Zheng, Q.-Y.; Fan, Q.-H. *J. Am. Chem. Soc.* **2009**, *131*, 7950−7951. (b) Liu, Z.-X.; Feng, Y.; Yan, Z.-C.; He, Y.-M.; Liu, C.; Fan, Q.-H. *Chem. Mater.* **2012**, *24*, 3751−3757. (c) Liu, Z.-X.; Feng, Y.; Zhao, Z.-Y.; Yan, Z.-C.; He, Y.-M.; Luo, X.-J.; Liu, C.-Y.; Fan, Q.-H. *Chem.—Eur. J.* **2014**, *20*, 533−541. (d) Zhao, G.-Z.; Chen, L.-J.; Wang, W.; Zhang, J.; Yang, G.; Wang, D.-X.; Yu, Y.; Yang, H.-B. *Chem.—Eur. J.* **2013**, *19*, 10094−10100.

(17) (a) Schenning, A. P. H. J.; Jonkheijm, P.; Peeters, E.; Meijer, E. W. *J. Am. Chem. Soc.* **2001**, *123*, 409−416. (b) Lee, E.; Kim, J.-K.; Lee, M. *Angew. Chem., Int. Ed.* **2009**, *48*, 3657−3660.

(18) (a) Wang, Y.; Xu, H.; Zhang, X. *Adv. Mater.* **2009**, *21*, 2849−2864. (b) Zhang, X.; Chen, Z.; Würthner, F. *J. Am. Chem. Soc.* **2007**, *129*, 4886−4887. (c) Wang, C.; Wang, Z.; Zhang, X. *Acc. Chem. Res.* **2012**, *45*, 608−618. (d) Ding, L.; Fang, Y. *Chem. Soc. Rev.* **2010**, *39*, 4258−4273. (e) Dong, S.; Luo, Y.; Yan, X.; Zheng, B.; Ding, X.; Yu, Y.; Ma, Z.; Zhao, Q.; Huang, F. *Angew. Chem.* **2011**, *123*, 1945−1949; *Angew. Chem., Int. Ed.* **2011**, *50*, 1905−1909. (f) Yan, X.; Wang, F.; Zheng, B.; Huang, F. *Chem. Soc. Rev.* **2012**, *41*, 6042−6045.

(19) (a) Giacomelli, C.; Schmidt, V.; Borsali, R. *Macromolecules* **2007**, *40*, 2148−2157. (b) Zhang, X.; Rehm, S.; Safont-Sempere, M. M.; Würthner, F. *Nat. Chem.* **2009**, *1*, 623−629.